Proceedings of the 21st ICSMGE, Vienna, Austria, 14 – 19 June 2026. Pistrol, Adam & Schweiger (eds.)
Published by: ÖGG, Austrian Society for Geomechanics, Salzburg, Austria, ISBN 978-3-9503898-4-5
https://doi.org/10.53243/ICSMGE2026-1049

Interaction effects in energy tunnels: A thermo-hydro-mechanical model incorporating small strain stiffness effects.

M. Julieta Rottemberg, Asal Bidarmaghz, Arman Khoshghalb.
School of Civil and Environmental Engineering, University of New South Wales, Australia,
m.rottemberg@student.unsw.edu.au

Alejo O. Sfriso.
Facultad de Ingenieria, University of Buenos Aires, Argentina.

ABSTRACT: Energy tunnels harness geothermal energy from the ground via embedded heat-exchange pipes, providing a sustainable solution for space heating, cooling, and hot water production. In dense urban environments, these systems are often built as twin tunnels to maximise thermal exchange area. However, when both tunnels are thermally activated, mutual thermal interference can occur, influencing ground temperature, pore pressure, and deformation patterns. This study applies a fully coupled thermo–hydro–mechanical (THM) modelling framework incorporating small-strain stiffness degradation within a critical state formulation to examine the long-term behaviour of twin energy tunnels under simultaneous thermal activation. The approach captures realistic soil stiffness evolution under excavation and cyclic thermal loading. The results show that thermal plumes from both tunnels merge over time, producing a broad thermal influence zone in the intervening soil. Cooling-induced volumetric contraction generates negative excess pore pressures, peaking in the first operational year before gradually dissipating over the long term. The mechanical response is characterised by seasonal cyclic settlements superimposed on a gradual downward trend, with the largest displacements occurring between the tunnels due to overlapping thermal influence zones. These findings highlight the importance of accounting for mutual thermal interference and fully coupled THM effects in design. Incorporating small-strain stiffness degradation improves the accuracy of predicted deformations and pore pressure changes, reducing the risk of overestimating thermal performance or underestimating long-term mechanical impacts. The proposed framework provides a robust basis for the safe and efficient design of twin energy tunnel systems.

KEYWORDS: Energy tunnels; thermo-hydro-mechanical behaviour; strain-dependent stiffness; geothermal energy; sustainability.

1 INTRODUCTION

Energy tunnels—tunnels equipped with heat-exchange pipes to function as shallow geothermal systems—present a promising solution to decarbonise urban heating and cooling by harnessing the thermal potential of subsurface infrastructure (Laloui and Loria, 2019). However, their widespread adoption is hindered by the complex thermo-hydro-mechanical (THM) interactions between the tunnel lining and the surrounding soil, particularly under cyclic thermal loading conditions.

Twin tunnel configurations are commonly adopted in urban settings for operational and spatial efficiency (Divall, Goodey et al., 2017). Thermally activating both tunnels can double the energy exchange surface but also leads to mutual thermal interference, where overlapping thermal plumes affect ground temperature fields, pore pressures, and stress redistribution. Despite their practical relevance, studies on twin energy tunnels remain scarce and report contradicting conclusions on the extent and nature of thermal and mechanical interactions (Gawecka, Cui et al., 2021, Liu and Zhou, 2023).

Most existing analyses on energy tunnels rely on simplified constitutive models that do not account for strain-dependent stiffness degradation, a key mechanism influencing soil response during excavation and thermal cycling (Mair, 1993). This can lead to inaccurate predictions of settlement, pore pressure evolution, and tunnel performance.

To address these gaps, this study employs a fully coupled THM model with small-strain stiffness degradation embedded in a critical state framework to investigate thermal interactions and the resulting mechanical behaviour of twin energy tunnels. The findings offer key insights into the design and performance of twin energy tunnels under realistic geotechnical conditions.

2 INCORPORATION OF SMALL STRAIN STIFFNESS

Strain-dependent stiffness degradation is incorporated into the model using simplified piecewise-linear degradation curves for both the shear modulus (G) and bulk modulus (K), which ensures computational efficiency and numerical stability. The shear modulus G varies with shear strain (γ) and is expressed as:

$$G = \begin{cases} G_{max} & \gamma \leq \gamma_{s1} \\ (a_s - b_s \cdot log(\gamma)) \cdot G_{max} & \gamma_{s1} < \gamma \leq \gamma_{s2} \\ G_{min} & \gamma > \gamma_{s2} \end{cases} \quad (1)$$

Similarly, the bulk modulus K is updated through a strain-dependent swelling index $\kappa(\varepsilon_v)$:

$$K = \frac{(1 + e_0)p'}{\kappa(\varepsilon_v)} \quad (2)$$

where e_0 is the initial void ratio and p' is the mean effective stress. The swelling index $\kappa(\varepsilon_v)$ increases with volumetric strain, progressively reducing the bulk stiffness as follows.

$$\kappa(\varepsilon_v) = \begin{cases} \kappa_{min} & \varepsilon_v \leq \varepsilon_{v1} \\ (a_v + b_v \cdot log(\varepsilon_v)) \cdot \kappa_{min}, & \varepsilon_{v1} < \varepsilon_v \leq \varepsilon_{v2} \\ \kappa_{max} & \varepsilon_v > \varepsilon_{v2} \end{cases} \quad (3)$$

3 FINITE ELEMENT IMPLEMENTATION

3.1 *Numerical setup and boundary conditions*

A numerical simulation is conducted to assess the thermo-hydro-mechanical (THM) response of a twin tunnel system excavated in soft ground and subjected to thermal loading using the (COMSOL Multiphysics, 2024) simulation platform. The model geometry, mesh, and boundary conditions are shown in Figure 1.

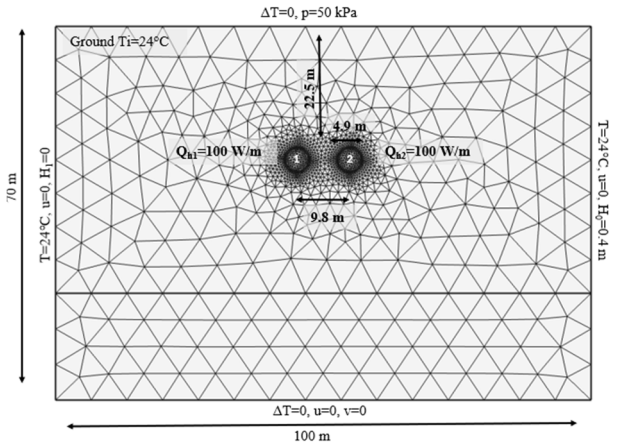

Figure 1. Finite element mesh and boundary conditions. Tunnel 1 and Tunnel 2 are subjected to thermal loads Q_{h1} and Q_{h2}.

Tunnel excavation is simulated in two stages: Tunnel 1 is excavated and supported first, followed by Tunnel 2. The convergence–confinement method is used to simulate excavation and support installation (Panet and Sulem, 2022). Initial in-situ stresses are generated via gravity loading. Excavation is represented by applying a uniform internal pressure mimicking TBM support, followed by partial pressure release to induce stress redistribution. The tunnel lining is then activated while removing the remaining pressure to simulate permanent support.

Mechanical boundary conditions include fixed displacements at the base (u=v=0) and horizontally restrained vertical sides (u=0), permitting vertical movement. A surface load accounts for overburden pressure. Hydraulic boundary conditions assume hydrostatic equilibrium with a horizontal head gradient imposed to induce groundwater flow. Vertical flow is restricted via no-flow boundaries at the top and bottom, and the tunnel linings are modelled as impermeable. Thermal boundary conditions assume an initial uniform ground temperature of T=24°C. Zero-flux thermal boundaries are applied laterally and at the base. A thermal load of $Q = 100$ W/mis applied along the tunnel linings, representing the simultaneous-activation scenario analysed in this study. The system operates under a cyclic thermal schedule consisting of 3-month activation periods followed by 3-month inactive periods, repeated twice per year.

3.2 *Twin tunnels and ground characteristics*

The soil profile and tunnel geometry are adapted from the well-documented San Francisco N–2 tunnel project, constructed in 1981 as part of the city's Clean Water Program (Abu-Farsakh and Voyiadjis, 1999, Clough, Sweeney et al., 1983). While the original case involved a single tunnel, the ground conditions, tunnel depth, and geometry have been modified to represent a hypothetical but realistic twin tunnel configuration suitable for studying thermal interaction effects. In the original project, transverse surface settlements were monitored and reached a maximum of about 30 mm, providing a useful reference for evaluating numerical predictions.

The subsurface consists of a 50 m thick layer of Bay Mud—a normally consolidated clay with low stiffness and high compressibility—underlain by stiffer colluvial deposits. Bay Mud is modelled using a Modified Cam–Clay formulation with strain-dependent stiffness degradation for shear and bulk moduli, while the colluvium is represented with a linear elastic–perfectly plastic Mohr–Coulomb model enhanced with similar stiffness degradation curves. Threshold values for the degradation functions are consistent with ranges reported in the literature for the onset of nonlinear soil behaviour under monotonic loading (Isenhower and Stokoe, 1981). The geotechnical parameters adopted are summarised in Table 1 and Table 2.

Table 1. Geotechnical properties and model parameters.

Material	Modified Cam–Clay model				Elastic and Mohr–Coulomb models		
	λ	κ	M	ν_1	c (kPa)	ρ (°)	K_0 (MPa)
Bay Mud	0.326	0.043	1.2	4.72	-	-	-
Colluvium	-	-	-	-	48	20	50

Table 2. Small Strain Stiffness model parameters.

Material	Small Strain Stiffness					
	G_{max} / G_{min}	γ_{s1}	γ_{s2}	κ_{max} / κ_{min}	ε_{v1}	ε_{v2}
Bay Mud	1.00E−05	1.00E−02	1.5	1.00E−03	1.00E−01	1.00E−05
Colluvium	1.00E−05	1.00E−02	1.5	1.00E−03	1.00E−01	1.00E−05

Thermal and thermo-mechanical properties, including effective thermal conductivity, specific heat capacity, thermal expansion coefficient, and hydraulic conductivity, are given in Table . These values are representative of typical clayey and granular soils and concrete tunnel lining, ensuring realistic simulation of heat transfer and thermally induced deformation (Gawecka, Cui et al., 2021, Laloui and Loria, 2019)

Table 3. Thermal and Thermo-Mechanical Properties.

Material	γ (kN/m³)	k_p (m/s)	λ_{eff} (W/mK)	C_p J/kgK)	Tf (°C)	α (1/K)
Bay Mud	17	1.00E-09	1.8	866	24	1.70 E-05
Colluvium	20	1.00E-05	2.2	850	24	3.30 E-06
Concrete	23	1.00E-09	1.8	880	-	1.00 E-05

Each tunnel has a circular cross-section with an external diameter of 4.9 m, a lining thickness of 0.3 m, and an internal diameter of 4.3 m. The crown is located at a depth of 22.5 m. The model domain spans 100 m in width and 70 m in height to minimise boundary effects, and a uniform 50 kPa surface surcharge is applied to account for traffic and infrastructure loads (Huang, Shao et al., 2017, Sieminska-Lewandowska and Mitew-Czajewska, 2007).

4 RESULTS

4.1 *Thermal response*

Figure 2 illustrates the spatial distribution of ground temperature surrounding the twin tunnel system at the end of the final cooling cycle for (a) year 1 and (b) year 20. The tunnels operate under a repeated thermal schedule of 3 months of activation followed by 3 months of inactivity. In year 1, the thermal influence zone remains localised around the linings, with limited overlap between the tunnels. By year 20, the

cooling plumes have expanded considerably, forming a merged thermal influence zone with pronounced temperature reductions in the intervening soil mass, indicating strong mutual thermal interference under long-term simultaneous activation.

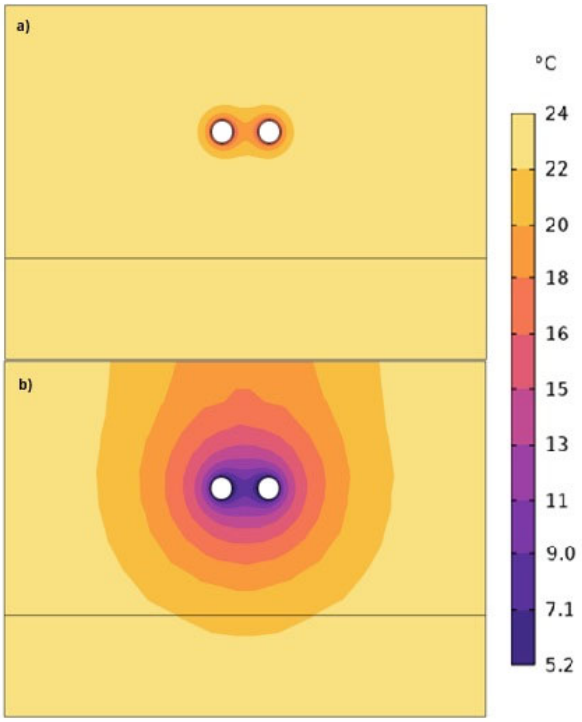

Figure 2. Spatial distribution of ground temperature surrounding the tunnel system at the end of the final cooling cycle for (a) year 1 and (b) year 20 of thermal operation.

4.2 *Hydraulic response*

Figure 3 shows the excess pore water pressure (Δu) distribution at the peak of the 3-month cooling cycle, corresponding to the maximum negative Δu that develops during the early stage of each cooling period, for (a) year 1 and (b) year 20. This response originates from the differential thermal contraction between the pore water and the soil skeleton. Specifically, the thermal expansion coefficient of water (α_w)is higher than that of the solid grains(α_s) and under undrained conditions, this mismatch leads to a net contraction of fluid volume, resulting in a rapid generation of negative excess pore pressures. This phenomenon has been widely observed in laboratory tests on clays (Burghignoli, Desideri et al., 2000, Hueckel and Pellegrini, 1992) In year 1, negative pore pressures are concentrated in the vicinity of the tunnel perimeters, with the maximum suction approaching approximately −20.5 kPa. By year 20 (Figure 3b), the peak magnitude reduces substantially to around −8 kPa, indicating long-term dissipation. Nevertheless, the spatial extent of the influence zone remains broader than in year 1, reflecting the cumulative thermal–hydraulic disturbance induced by repeated cooling cycles and the persistence of negative Δu in the intervening soil between the tunnels.

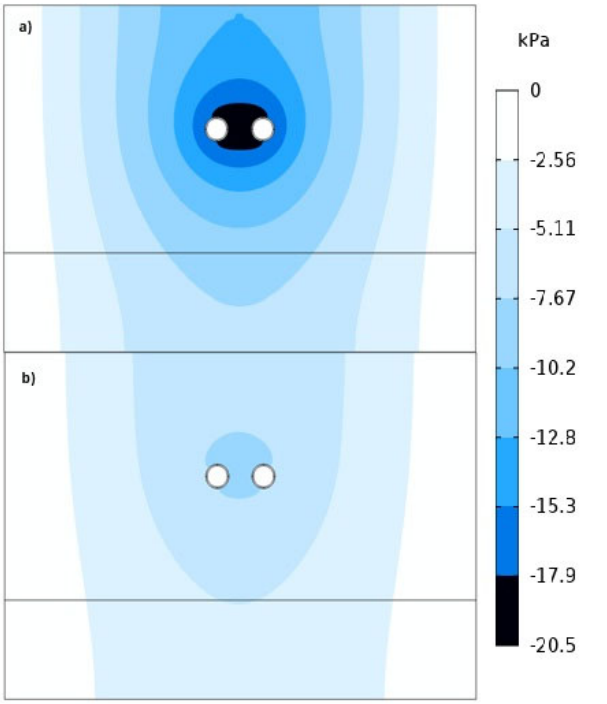

Figure 3. Contour plots of excess pore water pressure (Δu) around the twin tunnels at the peak of the cooling cycle—corresponding to the maximum negative Δu—during (a) year 1 and (b) year 20.

4.3 *Mechanical response*

Figure 4 shows the temporal evolution of vertical displacements at the ground surface over the 20-year period for monitoring points SF1 (above Tunnel 1), SF2 (above Tunnel 2), and SFM (midway between the tunnels). The response is characterised by a pronounced settlement during the first cooling cycle, after which the amplitude of cyclic movements gradually stabilises. The repeated thermal loading generates distinct seasonal settlement–rebound patterns superimposed on a long-term downward trend.

Due to the symmetrical and simultaneous activation of both tunnels, settlements at SF1 and SF2 remain nearly identical throughout the simulation. In contrast, the midpoint location SFM consistently exhibits the greatest cumulative settlement, highlighting the compounded effect of overlapping thermal influence zones and the mechanical interaction within the intervening soil mass. This behaviour reflects the combined influence of cooling-induced contraction, stiffness degradation, and the confinement conditions imposed by the twin tunnel geometry.

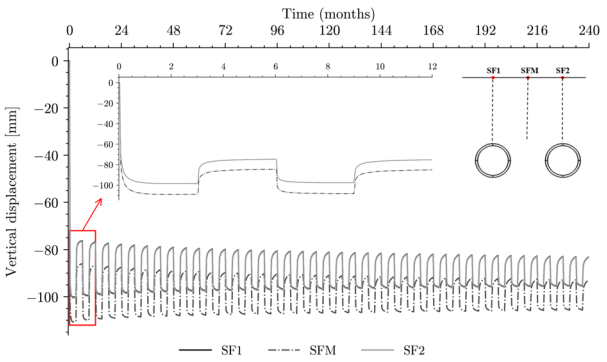

Figure 4. Temporal evolution of vertical displacements at the ground surface over a 20 year period. Results are shown for monitoring points

SF1 and SF2 (located above Tunnel 1 and Tunnel 2, respectively) and SFM (located midway between the tunnels). The inset highlights the response during the first year of thermal operation, illustrating the short-term cyclic behaviour.

5 CONCLUSIONS

This study examined the long-term thermo–hydro–mechanical (THM) behaviour of twin energy tunnels subjected to simultaneous thermal activation, using a fully coupled THM model that incorporates small-strain stiffness degradation within a critical state framework. The simulations revealed that cooling plumes from both tunnels progressively expand and merge over time, producing significant mutual thermal interference. This overlap alters the ground temperature distribution in the intervening soil and intensifies the coupled hydraulic and mechanical responses.

The hydraulic response was governed by the mismatch in thermal expansion coefficients between the pore water and the soil skeleton, generating negative excess pore pressures during cooling. Peak suctions occurred in the first operational year, with gradual dissipation over time, although the spatial extent of the influence zone remained broader due to repeated thermal cycling.

Mechanically, the system exhibited cyclic seasonal settlements superimposed on a long-term downward trend, with the largest displacements recorded at the midpoint between the tunnels. The inclusion of small-strain stiffness degradation was essential to accurately capture these deformations, preventing the overestimation that would result from simplified constitutive models.

Overall, the results highlight the importance of accounting for mutual thermal interference and fully coupled THM effects in the design of twin energy tunnels. Neglecting these interactions could lead to overestimation of thermal efficiency and underestimation of long-term settlements, potentially compromising structural integrity and the performance of adjacent infrastructure.

6 REFERENCES

Abu-Farsakh, M.Y. and Voyiadjis, G.Z. 1999. Computational model for the simulation of the shield tunneling process in cohesive soils. *International Journal for Numerical and analytical methods in Geomechanics* 23(1) 23-44.

Burghignoli, A., Desideri, A. and Miliziano, S. 2000. A laboratory study on the thermomechanical behaviour of clayey soils. *Canadian Geotechnical Journal* 37(4) 764-780.

Clough, G.W., Sweeney, B.P. and Finno, R.J. 1983. Measured soil response to EPB shield tunneling. *Journal of Geotechnical Engineering* 109(2) 131-149.

COMSOL Multiphysics 2024. COMSOL Multiphysics Reference Manual. Stockholm, Sweden, COMSOL AB.

Divall, S., Goodey, R. and Stallebrass, S. 2017. Twin-tunnelling-induced changes to clay stiffness. *Géotechnique* 67(10) 906-913.

Gawecka, K.A. et al. 2021. Predictive modelling of thermo-active tunnels in London Clay. *Géotechnique* 71(8) 735-748.

Huang, H., Shao, H., Zhang, D. and Wang, F. 2017. Deformational responses of operated shield tunnel to extreme surcharge: a case study. *Structure and Infrastructure Engineering* 13(3) 345-360.

Hueckel, T. and Pellegrini, R. 1992. Effective stress and water pressure in saturated clays during heating–cooling cycles. *Canadian Geotechnical Journal* 29(6) 1095-1102.

Isenhower, W.M. and Stokoe, K.H. 1981. Strain-rate dependent shear modulus of San Francisco Bay mud.

Laloui, L. and Loria, A.F.R. 2019. *Analysis and design of energy geostructures: theoretical essentials and practical application*: Academic Press.

Liu, J. and Zhou, C. 2023. Numerical investigation on the thermo-mechanical behaviour of twin energy tunnels. *Canadian Geotechnical Journal* 60(9) 1352-1369.

Mair, R. 1993. Developments in geotechnical engineering research: application to tunnels and deep excavations. Proc. Instn. Civ. Engrs. Civ. Engng.

Panet, M. and Sulem, J. 2022. *Convergence-confinement method for tunnel design*: Springer.

Sieminska-Lewandowska, A. and Mitew-Czajewska, M. 2007. Design of diaphragm walls according to EN 1997-1: 2004 Eurocode 7. Proceedings of the 14th European conference on soil mechanics and geotechnical engineering.